

# One-pot synthesis of CRBN PROTACs via photoinduced C(sp<sup>2</sup>)-C(sp<sup>3</sup>) cross coupling and amide formation for PROTAC library synthesis

Christine M. Arndt<sup>‡[a,b]</sup>, Jacqueline Bitai<sup>‡[a]</sup>, Jessica Brunner<sup>[a]</sup>, Till Opatz<sup>[b]</sup>, Paola Martinelli<sup>[a]</sup>, Andreas Gollner<sup>[a]</sup>, Kevin R. Sokol<sup>[a]</sup> and Matthias Krumb<sup>\*[a]</sup>

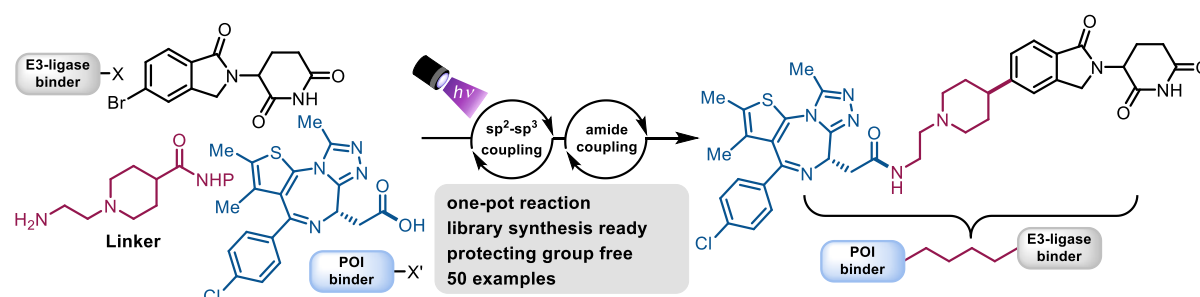
<sup>[a]</sup>Boehringer Ingelheim RCV GmbH & Co KG, Dr. Boehringer-Gasse 5-11, 1121 Vienna, Austria.

<sup>[b]</sup>Department of Chemistry, Johannes Gutenberg-University, Duesbergweg 10-14, 55128 Mainz, Germany.

<sup>‡</sup>Authors contributed equally

\*Corresponding author: matthias.krumb.chem@gmail.com.

## Graphical Abstract



## Abstract

In this study, a one-pot synthesis via photoinduced C(sp<sup>2</sup>)-C(sp<sup>3</sup>) coupling followed by amide formation to access proteolysis targeting chimeras (PROTACs) was developed. The described protocol was studied on cereblon (CRBN)-based E3-ligase binders and (+)-JQ-1, a bromodomain inhibitor, to generate BET (bromodomain and extra terminal domain) targeting protein degraders. The generated PROTACs were profiled in-vitro and tested for their degradation ability with several potent candidates identified. Upfront, the individual reactions of the one-pot transformation were carefully optimized for CRBN binder functionalization and multiple heterobifunctional linker moieties were designed and synthesized. Separate scopes detailing the C(sp<sup>2</sup>)-C(sp<sup>3</sup>) coupling and one-pot PROTAC synthesis are described in this report as well as a library minituarization study showing the high-throughput compatibility. Overall, the developed protocol provides rapid access to PROTACs in a single process thereby allowing efficient generation of CRBN-based PROTAC libraries.

## Introduction

The discovery of proteolysis targeting chimeras (PROTACs) and their ability to introduce proximity between an E3-ligase and a protein-of-interest (POI) opened up the toolbox of targeted protein degradation (TPD) in drug discovery.<sup>1,2</sup> This research area has been evolving and innovating with impressive speed over the last decade on both ends of academic research and pharmaceutical industry, with the first successful compounds now approaching investigational new drug (IND)-filing or even treatment of patients in the clinics.<sup>3</sup> TPD works via repurposing of the ubiquitin proteasome system (UPS), naturally responsible for the degradation of misfolded or dysfunctional proteins, and consisting of an ubiquitin activating enzyme (E1), ubiquitin conjugating enzyme (E2) as well as an E3-ligase. The latter transfers ubiquitin to the protein substrate to mark it for degradation via the proteasome.<sup>4</sup> Specific ligands binding to an E3-ligase can be combined with a POI inhibitor or binder connected via a linker moiety to form a heterobifunctional molecule, labeled as PROTAC. PROTACs were initially discovered by Crews and Deshaies already in 2001 and were subsequently further improved and developed by academic and industrial laboratories worldwide.<sup>5,6</sup> In contrast to classical

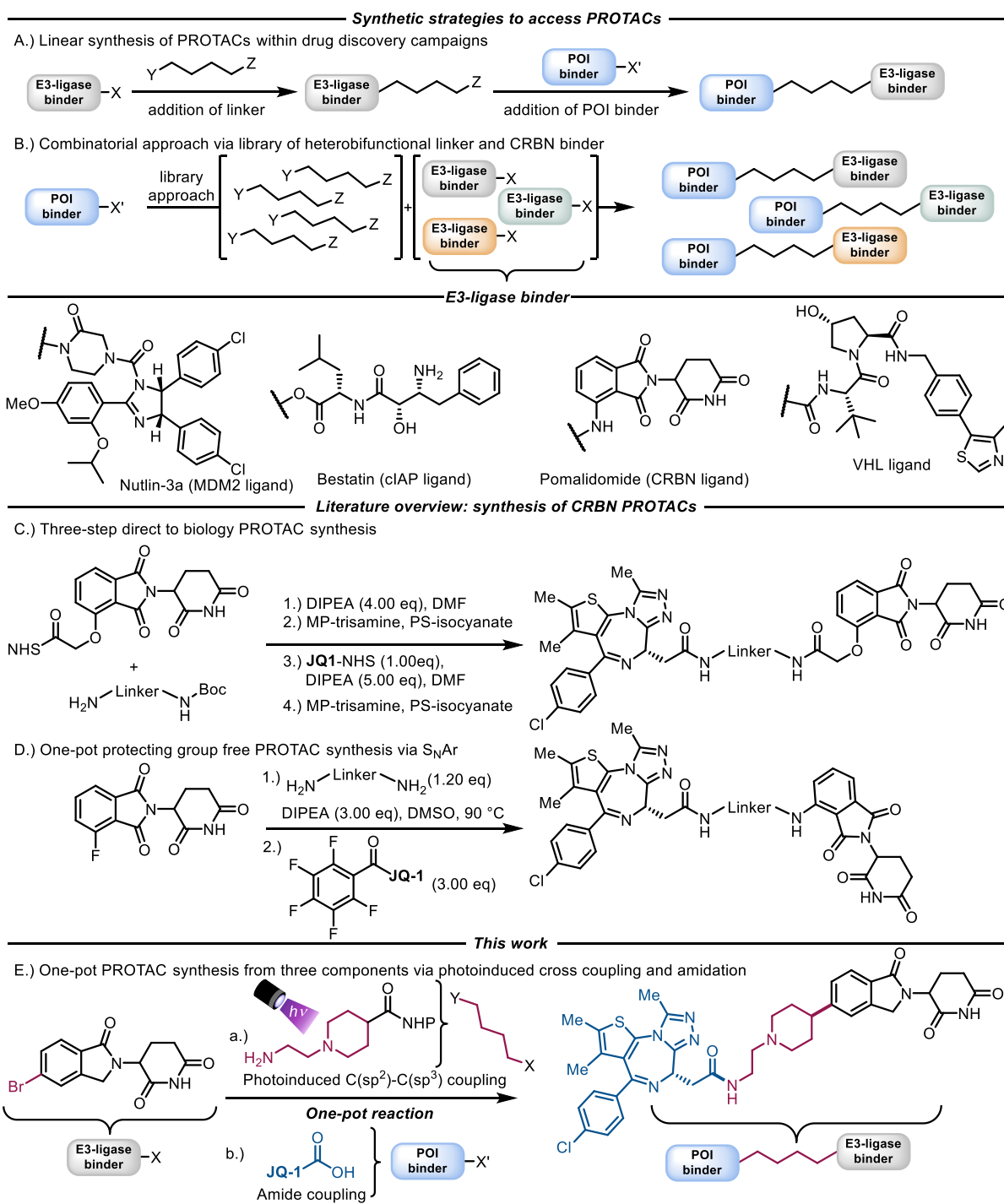
inhibitors, PROTACs exhibit distinct advantages rendering them attractive for drug discovery, such as their catalytic mode of action in the cell. This concept also allows the targeting of classical undruggable targets for which inhibitors do not exist, as it relies on degradation rather than inhibition.<sup>7</sup>

The current strategy to synthesize PROTACs often starts with an E3-ligase binder, which is subsequently functionalized with a linker building block (BB) to form a monofunctional PROTAC precursor (Scheme 1, A).<sup>8</sup> The latter is then combined with a POI binder to form a single PROTAC, which is subsequently profiled in *in-vitro* and potentially in *in-vivo* settings. Although recently the rational design of protein degraders has made significant progress via structure-based design from ternary complex crystal or CryoEM structures, the vast majority of optimization efforts by medicinal chemists still proceeds via empirical design cycles.<sup>9,10</sup> In fact, this leads to an explicitly high number of PROTACs needing to be synthesized for hit finding or lead optimization during protein degrader projects.<sup>11</sup> This represents a current bottleneck for protein degrader programs, thereby prolonging timelines to the clinics unnecessarily. Thus, there is a significant scientific need to improve the synthetic access to PROTAC molecules with the aim of accelerating drug discovery campaigns in pharmaceutical industry. Fortunately, pioneering reports in literature started to improve this tedious process by moving towards library-based approaches and miniaturizing PROTAC synthesis for high throughput settings (Scheme 1, B). In these libraries, binders for the E3-ligases von Hippel-Lindau (VHL), cereblon (CRBN), inhibitor of apoptosis protein (IAP) and mouse double minute 2 homolog (MDM2) are the most frequently used,<sup>12</sup> with a current clear focus on CRBN-based PROTACs. This can be explained when comparing the molecular properties of these E3-ligase binders, where CRBN ligands are the most drug-like and therefore furnish PROTACs closest to the desired rule-of-five or beyond rule-of-five chemical space.<sup>13</sup>

An intriguing example among recent reports is the direct-to-biology approach by Hendrick et al., which used a library of *N*-Boc diamine linkers in combination with carboxylic acid based POIs and CRBN binders (Scheme 1, C).<sup>14</sup> The combination of a POI binder with a matrix of bifunctional linker moieties and an E3-ligase binder offers an attractive alternative to previously mentioned linear and therefore tedious synthesis strategies (Scheme 1, B).<sup>15</sup> Besides literature known reports, both one-pot and multicomponent reactions seem in general feasible to combine a POI binder, an E3-ligase binder and a heterobifunctional linker to form diverse libraries of PROTACs, specifically when resin based approaches are not feasible.<sup>16</sup> Although multicomponent reactions (MCRs), such as the Strecker, Petasis, Biginelli or Ugi reaction are robust and well-studied, they offer only limited potential to introduce geometrically and structurally diverse molecular architectures in the linker moiety.<sup>8,17</sup> However, these diverse changes in the linker are required to optimize degradation and DMPK properties of the final PROTAC molecules.<sup>18</sup> Nevertheless, Pirali and coworkers were able to develop such an MCR protocol for the synthesis of BRD4 degrading PROTACs via Ugi and Passerini reactions using CRBN and VHL-based ligands for degradation.<sup>19</sup> Besides MCRs, one-pot transformations should allow faster access to PROTACs, minimalizing the number of work-up and purification steps, thereby reducing chemical waste. Thus, they seem particularly attractive for library-based approaches.<sup>20</sup> This envisioned one-pot transformation needs to combine a heterobifunctional linker with a POI binder and an E3-ligase binder in a well optimized reaction, assembling the desired structure in a feasible yield with minimized side product formation. A practical example of such an approach was studied by Derksen and coworkers, investigating the synthesis of pomalidomide conjugates via  $S_NAr$  and amidation reactions (Scheme 1, D).<sup>21</sup> However, one limitation of the studied method is the requirement of using heteroatom rich amino linkers for functionalization of the E3-ligase binder as well as the employed nucleophilic aromatic substitution, which is known to only work on thalidomide derivatives, limiting the portfolio of CRBN binders applicable.<sup>22</sup>

In view of these pioneering literature findings, we sought to expand the current toolbox of protocols for one-pot PROTAC synthesis with the aim to accelerate our in-house protein degrader programs and provide a robust method that utilizes bench-stable precursors and mild reaction conditions with broad functional group tolerance (Scheme 1, E). We envisioned the connection of the linker to the E3-ligase binder via C(sp<sup>2</sup>)-C(sp<sup>3</sup>) coupling, followed by an amide coupling to connect the carboxylic acid-based POI binders. This strategy grants more structural flexibility regarding the linker moiety, specifically allowing access to rigidified carbocycles within the linker to reduce conformational flexibility as well as number of rotatable bonds. In addition, the introduction of carbocycles allows for a reduction in the number of heteroatoms and H-bond donors within the linker,<sup>23</sup> which was a specific limitation for us using literature methods, which yield PROTACs quite far from the drug-like PROTAC chemical space (Scheme 1, C and D).<sup>24</sup> The utilized amide coupling was chosen for this one-pot transformation as it is well studied and many robust protocols with broad functional group tolerance and bench-stable precursors are available.<sup>25</sup>

For the C(sp<sup>2</sup>)-C(sp<sup>3</sup>) cross coupling we selected a range of literature methods with a specific focus on photoinduced reactions, as these not only offer rather unique modes of reactivity with access to C(sp<sup>2</sup>)-C(sp<sup>3</sup>) disconnections orthogonal to many other chemistries, but also exceptionally mild reaction conditions to tolerate sensitive functional groups.<sup>26-30</sup> The latter is specifically important when studying CRBN PROTACs since the majority of CRBN ligands utilize a glutarimide moiety to bind into the thalidomide-binding pocket (TBD) of CRBN.<sup>13</sup> These glutarimides are intrinsically prone to epimerization and hydrolysis of the imide functional group.<sup>31,32</sup> Therefore, careful selection of reaction conditions is needed to functionalize the CRBN binding moiety. Finally, we chose (+)-JQ-1, a BET (bromodomain and extra terminal domain) inhibitor as the model POI binder, since BET degraders are not only well studied, but also allow comparison of the herein developed protocol with the previously published reports.<sup>33</sup>



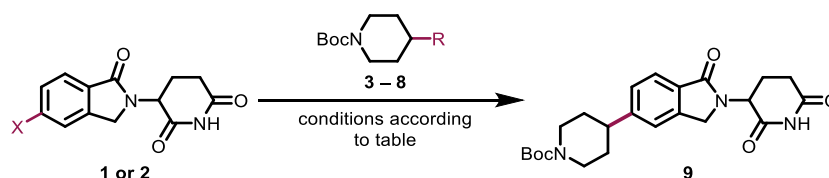
**Scheme 1:** Depiction and literature overview of synthetic strategies to access PROTACs. A.) Linear synthesis strategy to access PROTACs from single a E3-ligase binder connected with a linker BB and a POI binder. B.) Combinatorial approach for PROTAC synthesis via a matrix of heterobifunctional linkers as well as E3-ligase binders. Depiction of commonly used E3-ligase binders below for MDM2, IAP, CRBN and VHL. C.) Direct to biology PROTAC synthesis via three steps described by Hendrick and coworkers.<sup>14</sup> D.) Protecting group free one-pot PROTAC synthesis via tandem  $S_NAr$  and amide coupling by Derksen and coworkers.<sup>21</sup> E.) Herein developed protocol for one-pot photoinduced  $C(sp^2)-C(sp^3)$  coupling and amide formation to synthesize CRBN PROTACs from a CRBN ligand, bifunctional linker, and POI binder. NHS = N-hydroxysuccinimide NHP = N-hydroxyphthalimide.

## Main text

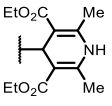
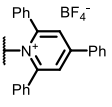
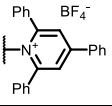
The envisioned one-pot process to access CRBN-based PROTACs starts with a C(sp<sup>2</sup>)-C(sp<sup>3</sup>) cross coupling between a CRBN ligand and a heterobifunctional linker moiety (Scheme 1, E). We selected a range of published protocols with a diverse palette of cross coupling precursors to study the functionalization of CRBN binder **1**,<sup>34-37</sup> an aryl bromide derivative of the CRBN binder lenalidomide.<sup>38</sup> Specifically, we selected trifluoroborates<sup>39,40</sup>, alkyl halides<sup>41</sup>, 1,4-dihydropyridines<sup>42</sup>, carboxylic acids<sup>43</sup>, redox active esters<sup>44</sup>, as well as pyridinium salts<sup>45,46</sup> as suitable coupling partners (Table 1). First, we investigated the ability of trifluoroborates for the envisioned C(sp<sup>2</sup>)-C(sp<sup>3</sup>) coupling as described by Molander and coworkers.<sup>39,40</sup> Unfortunately, neither the alkylboron coupling catalyzed by palladium (Entry 1), nor the photoredox catalysis conditions (Entry 2) showed notable product formation. Similar results were obtained with the coupling of 1,4-dihydropyridines described by Melchiorre and coworkers<sup>42</sup> (Entry 4) and pyridinium salts described by Molander and coworkers (Entry 8).<sup>46</sup> In contrast, productive reactivity was observed upon coupling alkyl bromides using the protocol by MacMillan and coworkers<sup>41</sup> with 10% yield (Entry 3) or using carboxylic acids described in a subsequent protocol by MacMillan and coworkers<sup>43</sup> resulting in 15% yield (Entry 5). A higher initial yield was observed upon coupling of redox active esters employing a protocol by Molander and coworkers<sup>44</sup> with 22% yield (Entry 6). Coupling of pyridinium salts using a method developed by Koh and coworkers also proved to be successful with 36% yield (Entry 7).<sup>45</sup> Interestingly, the method by Molander and coworkers<sup>46</sup> facilitating the reductive coupling of pyridinium salts with 4CzIPN as photocatalyst resulted in no product formation (Entry 8), whereas the method detailed by Koh and coworkers<sup>45</sup> employing Hantzsch ester as a photoreductant proved successful and the product was isolated in 22% yield (Entry 6).

After evaluation of the literature protocols, the method developed by Molander and coworkers<sup>44</sup> using redox active esters was selected for further investigation due to the ease of synthesis of redox active esters as radical precursors from carboxylic acids and their broad commercial availability. Moreover, the simple reaction conditions utilizing Ni(dtbbpy)Br<sub>2</sub> and Hantzsch ester as the only additional reagents in DMA under purple LED irradiation to facilitate the desired C(sp<sup>2</sup>)-C(sp<sup>3</sup>) coupling was a clear benefit compared to other methods. Noteworthy, this reaction proceeds via electron-donor-acceptor (EDA) complex formation without the need for a transition metal-based catalyst rendering this process sustainable and amenable for library generation.<sup>47,48</sup>

**Table 1:** Investigation of literature methods onto the C(sp<sup>2</sup>)-C(sp<sup>3</sup>) cross coupling of glutarimide derivative **1** or **2**. See supporting information for full details on reaction conditions. All yields shown are isolated yields. N.d. = not detected.

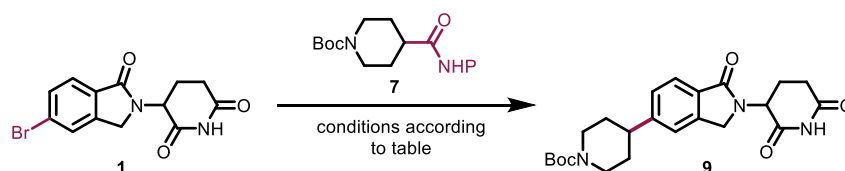


Entry	Literature	X	R	Yield [%]
1	Molander <i>et al.</i> <sup>39</sup>	Br	BF <sub>3</sub> K	n.d.
2	Molander <i>et al.</i> <sup>40</sup>	Br	BF <sub>3</sub> K	n.d.
3	MacMillan <i>et al.</i> <sup>41</sup>	Br	Br	10

4	Melchiorre <i>et al.</i> <sup>42</sup>	Br		n.d.
5	MacMillan <i>et al.</i> <sup>43</sup>	I	CO <sub>2</sub> H	15
6	Molander <i>et al.</i> <sup>44</sup>	Br	CO <sub>2</sub> NHP	22
7	Koh <i>et al.</i> <sup>45</sup>	Br		36
8	Molander <i>et al.</i> <sup>46</sup>	Br		n.d.

After selection of a suitable method, we carried out optimization studies to improve the conditions for functionalization of CRBN binder derivative **1** (Table 2). Since the method by Molander and coworkers<sup>44</sup> uses EDA complex photoactivation, the influence of different solvents and reaction concentration was examined first.<sup>49</sup> Interestingly, a range of different solvents were tolerated (see supporting information for details), but no further improvement over the initially selected DMA was identified (Entry 1). Notably, 1,4-dioxane showed significant conversion to the desired product **9** yielding a product/standard ratio of 0.26 (Entry 2). While changes in Hantzsch ester loading showed no further improvement (Entry 3), decreasing the equivalents of redox active ester (RAE **7**) from 2.00 to 1.50 equivalents improved conversion to the desired product (Entry 4). Screening of different Nickel catalysts (see supporting information for details) as well as catalyst loading revealed significant improvements when 0.50 equivalents were used (Entry 5). Finally, the robustness of the developed protocol was tested and various acids as well as base additives were evaluated (see supporting information for details). Much to our surprise, addition of 4.00 equivalents of NaHCO<sub>3</sub> raised the conversion to the desired product **9** with an observed product/standard ratio of 1.16 (Entry 7). Overall, the initial isolated yield was increased from 22% (Entry 1) to 69% (Entry 7) during the course of our optimization cycles.

**Table 2:** Optimization of the photoinduced C(sp<sup>2</sup>)-C(sp<sup>3</sup>) coupling originally described by Molander and coworkers.<sup>44</sup> [a]Standard conditions: aryl bromide **1** (1.00 eq), redox active ester **7** (2.00 eq), Ni(dtbbpy)Br<sub>2</sub> (10 mol%), HE (2.00 eq), DMA (0.1 M), rt, 24 h, purple LEDs (390 nm) [b]P/Std indicates product/ internal standard ratio (see supporting information for details). All yields are isolated yields.



Entry	Deviation from standard conditions <sup>[a]</sup>	(P/Std) <sup>[b]</sup> / Yield [%]
1	None	0.41 / 22
2	1,4-Dioxane (0.1 M)	0.26
3	HE (4.00 eq)	0.30
4	RAE <b>7</b> (1.50 eq)	0.65

5	RAE <b>7</b> (1.50 eq) + NiBr <sub>2</sub> (dtbbpy) (0.50 eq)	0.89
6	RAE <b>7</b> (1.50 eq) + Ni(acac) <sub>2</sub> (0.50 eq)	0.19
7	RAE <b>7</b> (1.50 eq) + NiBr <sub>2</sub> (dtbbpy) (0.50 eq) + NaHCO <sub>3</sub> (4.00 eq)	1.16 / <b>69</b>

With optimized conditions in hand, the scope of the developed reaction was investigated on a broad array of redox active esters derived from commercial carboxylic acid derivatives (Scheme 2). At first, primary (**16**) and secondary (**17**) radical precursors were reacted under the optimized reaction conditions, furnishing the desired products **46** and **47** in 65% and 86% isolated yields, respectively. As expected, tertiary radical precursor **18** did not show any product formation. On the other hand, tertiary alkyl carboxylic acids present in bridgehead systems such as bicyclo[2.2.2]octane (**19**) and adamantane (**20**) smoothly participated in this coupling to generate products with quaternary carbon centers (**49**, **50**). This finding is in line with earlier reports describing the difficulty of cross coupling unstrained tertiary radicals in Nickel photoredox catalyzed reactions.<sup>50</sup> Noteworthy, even cyclopropyl radicals (**21**), known to undergo radical-based side reactions,<sup>51</sup> successfully underwent the coupling with lenalidomide derivative **1** as shown by example **51**. Four to seven-membered aliphatic rings (**22** – **25**) also participated in the C(sp<sup>2</sup>)-C(sp<sup>3</sup>) cross coupling, forming the desired products (**52-55**) in up to 82% yield.

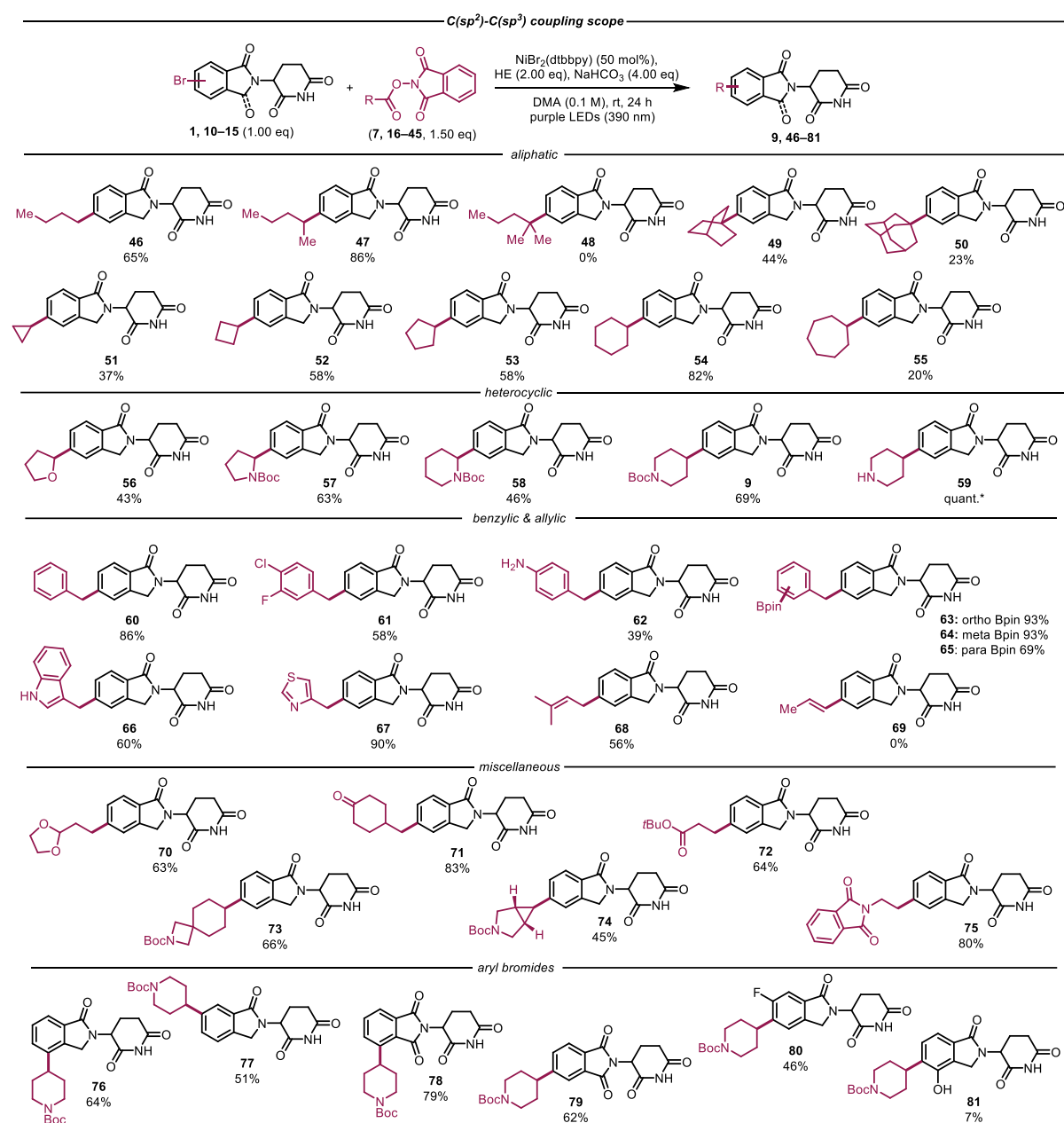
After various sources of alkyl radicals were investigated, we turned our attention to the reactivity of stabilized radical precursors such as benzylic,  $\alpha$ -amino or  $\alpha$ -oxy radicals.<sup>52,53</sup> Tetrahydrofuran **26** as oxygen containing heterocycle furnished the desired product **56** in 43% yield. Boc protected nitrogen heterocycles like pyrrolidine **27**, and piperidine **28** and **7** yielded the desired Boc-protected products **57**, **58** and **9** in up to 69% yield. An unprotected piperidine **29** was also well tolerated, furnishing the free amine product **59** (see supporting information for further details).

Benzylic radical precursors, both unfunctionalized (**30**) as well as with halogenated aromatic moieties (**31**) or aniline **32** showed similar conversion, underlining the robustness and functional group tolerance of the protocol. Furthermore, *ortho* (**63**), *meta* (**64**) and *para* (**65**) benzylic boronic esters were obtained in excellent 69-93% yield, as potential building blocks for further Suzuki cross coupling reactions. Finally, heterocycles such as indole **66** and thiazole **67** were obtained in good 60% and 90% yield, respectively. Interestingly, the use of a carboxylic acid precursor with an allylic quaternary center (**38**) resulted in the exclusive formation of rearranged alkene product **68** in 56% yield, which might occur via the formation of an allylic radical. In contrast, the formation of sp<sup>2</sup>-centered radicals as in **39** is not feasible, resulting in no product formation.

Additional functional groups like acetal **70**, ketone **71** and ester **72** were well tolerated under the used conditions, allowing quick access to further derivatization such as reductive amination or amide coupling after deprotection. In addition, rigidified 4,6-spirocyclic **43** and azabicyclo[3.1.0]hexane **44** furnished the desired products **73** and **74** in 66% and 45% isolated yield, respectively.<sup>54,55</sup>

Different regioisomers and derivatives of CRBN binding ligands were investigated next. Both aryl bromide regioisomers of lenalidomide showed comparable yields, furnishing the desired products **76** and **77** in 64% and 51%, respectively. In addition, thalidomide-based aryl bromide regioisomers showed excellent reactivity, giving the desired products with 79% (**78**) and 62% (**79**). Using a fluorinated lenalidomide derivative resulted in a slightly lower yield of 43% (**80**), whereas a phenolic lenalidomide yielded the product **81** only in 7% yield. These findings are particularly useful when

different exit vectors and linker geometries are screened in the course of a PROTAC drug discovery program to optimize a PROTAC's degradation and DMPK properties.<sup>56,57</sup>



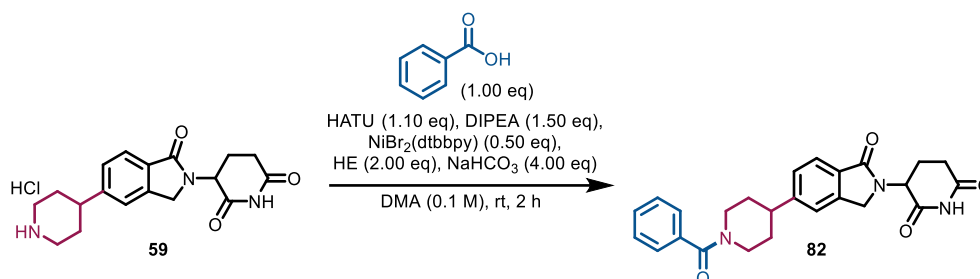
**Scheme 2:** Scope of the developed  $C(sp^2)-C(sp^3)$  cross coupling reaction. All yields are isolated yields. Reaction conditions: aryl bromide (1.00 eq), redox active ester (1.50 eq),  $\text{NiBr}_2(\text{dtbbpy})$  (50 mol%), Hantzsch ester (2.00 eq),  $\text{NaHCO}_3$  (4.00 eq), DMA (0.1 M), rt, 24 h, purple LEDs (390 nm). \*isolated as crude (see SI for details).

After successful optimization and evaluation of the  $C(sp^2)-C(sp^3)$  cross coupling reaction, we turned our attention towards the development of suitable reaction conditions for the envisioned follow-up amide coupling of the obtained CRBN binder linker conjugate with a suitable POI binder (Scheme 1, E). As a suitable model substrate, we chose piperidine derivative **59** and investigated amide coupling with benzoic acid using HATU and DIPEA in the presence of the remaining reaction components from the photoinduced  $C(sp^2)-C(sp^3)$  cross coupling (Table 3, entry 1). We observed successful product formation with a product/standard ratio of 0.87, translating into 62% isolated yield. Gratifyingly, no significant interference of the added  $\text{NiBr}_2(\text{dtbbpy})$ , Hantzsch ester or  $\text{NaHCO}_3$  was found. Next, different amide coupling reagents and additives were investigated (see the supporting information for



full details).<sup>25</sup> It was found that addition of HOBt improved the product/standard ratio for all coupling reagents tested (entry 2–4),<sup>58–60</sup> with HATU remaining the most favorable (entry 3). Different amine bases were tested subsequently, and it was found that both triethyl amine (TEA, entry 5) and 2,6-lutidine (entry 6) resulted in increased product formation over the initially used DIPEA. The latter case, 2,6-lutidine, showed the best product/standard ratio of 1.68 within the series and resulted in 80% yield of the desired product **82**.

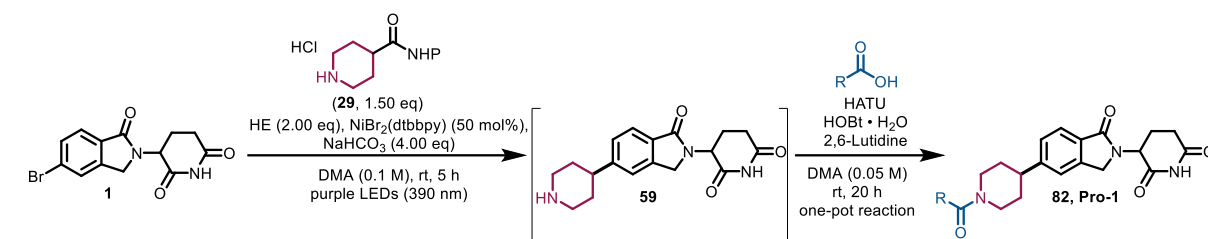
**Table 3:** Optimization of amide coupling towards one-pot PROTAC synthesis. <sup>[a]</sup>Standard conditions: amine **59** (1.00 eq), benzoic acid (1.00 eq), HATU (1.10 eq), DIPEA (1.50 eq), NiBr<sub>2</sub>(dtbbpy) (0.50 eq), HE (2.00 eq), NaHCO<sub>3</sub> (4.00 eq), DMA (0.1 M), rt, 2 h. <sup>[b]</sup>P/Std indicates product, internal standard ratio (see supporting information for details). All yields are isolated yields.

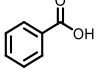
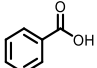
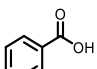
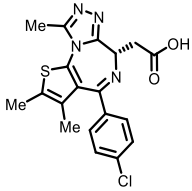
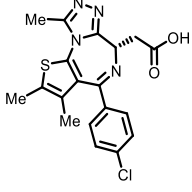


Entry	Deviation from standard conditions <sup>[a]</sup>	(P/Std) <sup>[b]</sup> / Yield [%]
1	None	0.87 / 62
2	EDC + HOBt (1.10 eq)	1.31
3	HATU + HOBt (1.10 eq)	1.61
4	TBTU + HOBt (1.10 eq)	0.91
5	HOBt (1.10 eq) + TEA (1.50 eq)	1.50
6	HOBt (1.10 eq) + 2,6-Lutidine (1.68)	1.68 / 80

After establishing optimal conditions for the C(sp<sup>2</sup>)–C(sp<sup>3</sup>) coupling as well as the amide coupling, we next investigated the applicability towards a one-pot transformation (Table 4). In an initial experiment, CRBN ligand **1**, piperidine derivative **29** and benzoic acid were combined in a one-pot protocol (Entry 1). Gratifyingly, the desired reaction was observed, and the product was isolated in 25% initial yield. Using higher equivalents of acid coupling partner and coupling reagents further raised the yield to 84% (entry 2). An additional increase to 10 equivalents benzoic acid (entry 3) instead of 2.5 (entry 2) indicated that no more improvement could be made. Since benzoic acid is a simple model substrate, we investigated the coupling of (+)-JQ-1 next (entry 4). The product could be isolated with a comparable yield of 70%, highlighting the robustness and functional group tolerance of the developed one-pot transformation. An additional increase in equivalents of the acid showed again no improvement in product yield, consistent with the results observed for benzoic acid as a model substrate (entry 3 vs 5).

**Table 4:** Optimization of the one-pot PROTAC synthesis towards model PROTAC **Pro-1**. All yields are isolated yields. See supporting information for full details.

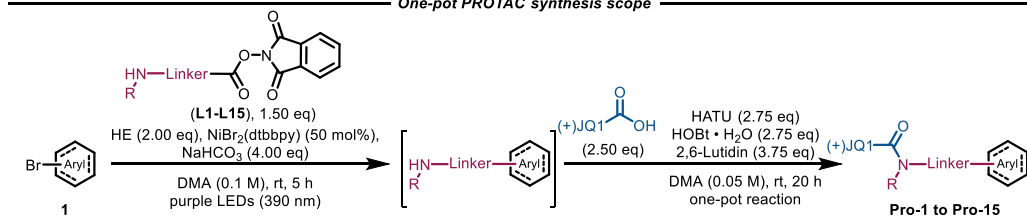


Entry	Carboxylic acid [eq]	HATU [eq]	HOBT [eq]	2,6-Lutidin [eq]	Yield [%]
1	 1.00	1.10	1.10	1.50	25
2	 2.50	2.60	2.60	3.00	84
3	 10.0	10.0	10.0	10.0	70
4	 2.50	2.75	2.75	3.75	70
5	 5.00	5.50	5.50	7.50	68

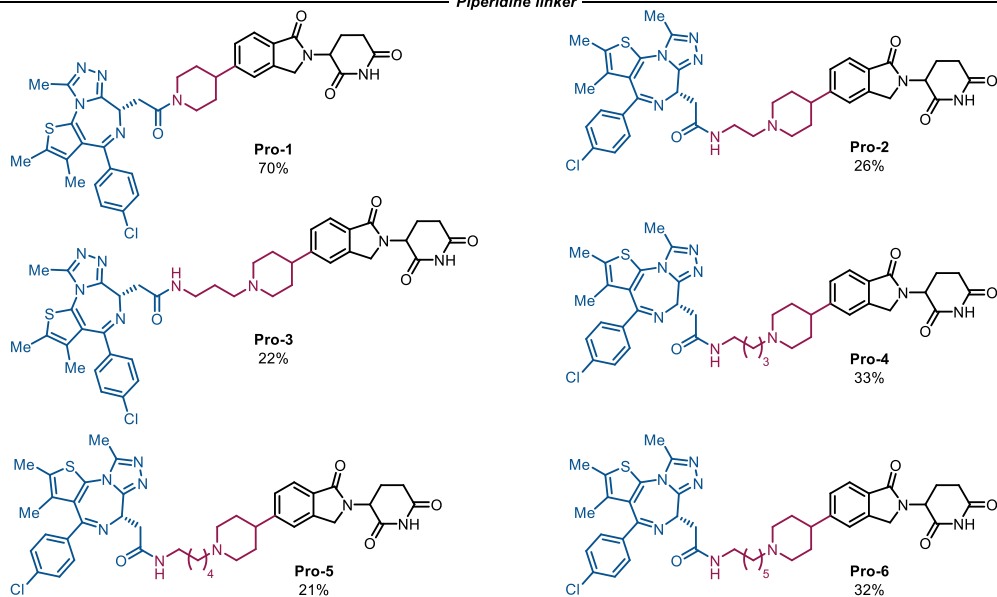
With optimized conditions for the one-pot transformation in hand, we next investigated the applicability of the developed protocol for the synthesis of various BET-targeting PROTACs (Scheme 3). In initial experiments, we reacted several bifunctional piperidine containing linkers of varying linker length with CBRN ligand **1** and (+)-JQ-1. Product formation was observed in all cases with the initial piperidine containing coupling partner giving the highest yield of 70% for the desired PROTAC **Pro-1**. Linker length variation and coupling of primary amines showed reduced but consistent yields ranging from 22–33% for PROTACs **Pro-2** to **Pro-6**.

Subsequently, several phenyl containing linkers were evaluated with stabilized, benzylic radicals formed in the photoinduced C(sp<sup>2</sup>)-C(sp<sup>3</sup>) coupling. Consistent and moderate yields were observed for PROTACs **Pro-7** to **Pro-12**, only showing a slight trend for decreasing yields with increasing linker length. Finally, rigidified structures featuring previously investigated spirocycles or conjugated cyclic systems were tested. For these examples moderate yields were observed, giving the desired products **Pro-13** to **Pro-15** with 27%, 37% and 27%, respectively.

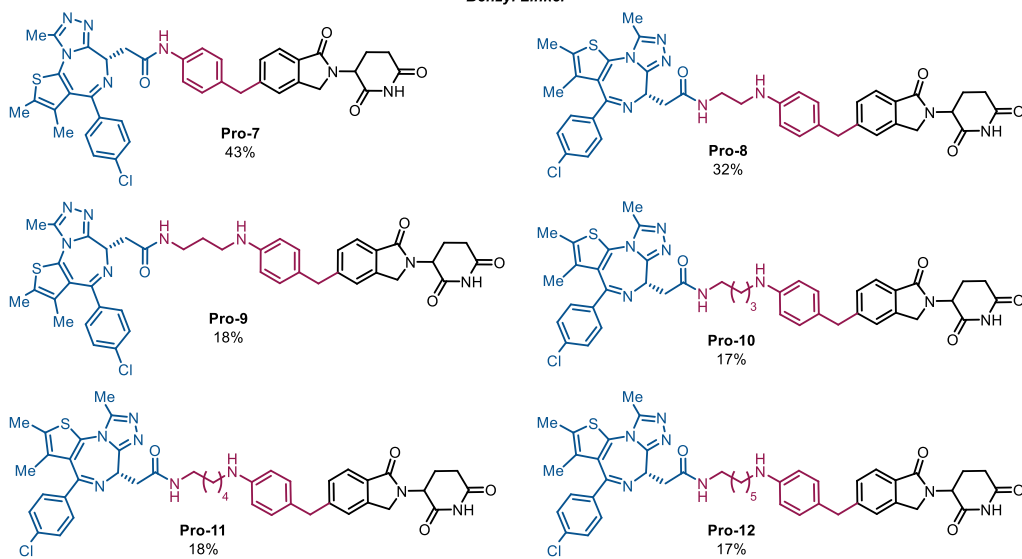
One-pot PROTAC synthesis scope



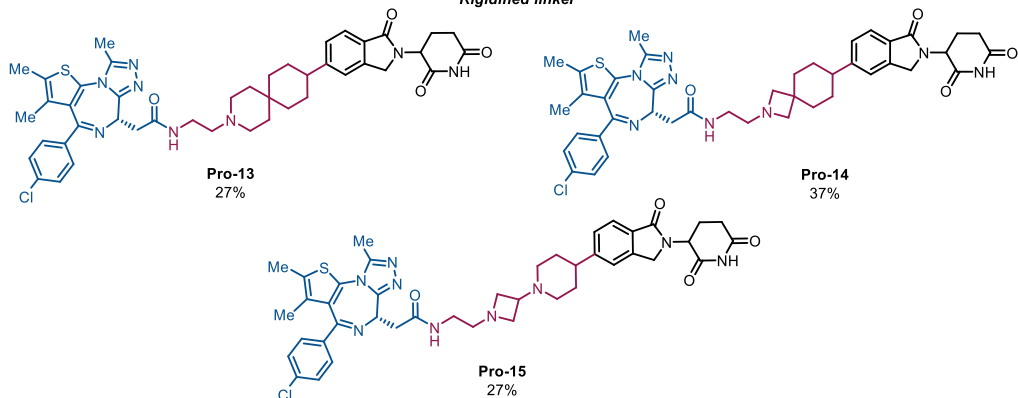
Piperidine linker



Benzyl Linker



Rigidified linker



**Scheme 3:** Scope of the developed one-pot PROTAC synthesis. All yields are isolated yields. See supporting information for full details on reaction conditions.

With several CRBN-(+)-JQ-1 PROTACs synthesized, we next turned our attention towards the *in-vitro* characterization of the obtained compounds (Table 5). At first, we tested the compounds for BRD4 degradation using HEK293 cells where the endogenous BRD4 had been tagged with HiBiT via CRISPR.<sup>61</sup> BRD4 levels were measured after treatment at different time points (4h and 18h). Gratifyingly, 14 out of these 15 tested compounds showed successful degradation of BRD4 with the most potent compound **Pro-6** showing a DC<sub>50</sub> (half maximal degradation concentration) of 0.7 nM or 0.3 nM and a D<sub>max</sub> (maximum level of target degradation) of 92% or 98% after 4h or 18h, respectively. A broad set of control experiments was performed for a subset of 5 compounds. In all cases, degradation was fully rescued by co-treatment with inhibitors of the proteasome (MG132 10 μM) or NEDD8 (MLN-4924 500 nM). Additionally, competition with either BRD4 binder ((+)-JQ-1 10 μM) or CRBN binder (lenalidomide 50 μM) also completely abrogated degradation (see supporting information Figure S2). Altogether, these data strongly indicate that BRD4 degradation induced by the CRBN-(+)-JQ-1 PROTACs is fully on-target.

Since CRBN-based PROTACs are known to induce the recruitment of off-target neosubstrates upon binding to CRBN, we tested for degradation of GSTP1, a well-described off-target of CRBN PROTACs, via another HiBiT-based assay in HEK293 cells.<sup>2,62,63</sup> Fortunately, no significant GSPT1 degradation was observed for all compounds tested (see the supporting information for details). Binding of the lenalidomide-based CRBN binder, which was used for the synthesis of the CRBN-(+)-JQ-1 PROTACs, was investigated via TR-FRET assay next. With the exception of **Pro-1**, the tested PROTACs **Pro-2** to **Pro-15** showed an IC<sub>50</sub> ranging from 36–79 nM. The outlier **Pro-1**, which had an about six fold higher IC<sub>50</sub>, could be explained by the very short linker moiety used, possibly already indicating steric clashes with the CRBN protein upon binding to the thalidomide-binding pocket.

Interestingly, trends in BRD4 degradation can be observed from comparison of the linker length between the synthesized series. For the piperidine linker containing PROTACs (**Pro-1** to **Pro-6**) a clear positive, downwards trend for the DC<sub>50</sub> can be observed ranging from 11.4 nM (**Pro-2**) to 0.3 nM (**Pro-6**) with the exception of compound **Pro-1** showing a DC<sub>50</sub> of 3.6 nM already with a very short and rigid linker moiety. Compounds **Pro-1** and **Pro-6** show a virtually similar IC<sub>50</sub> in our CRBN NanoBRET target-engagement assay in live and in permeabilized cells indicating proper permeability and potency of the synthesized PROTACs. Longer linkers, such as in **Pro-2** to **Pro-5** showed a larger shift between the live and permeabilized cells thereby suggesting minor permeability problems.

Similar trends as in the piperidine series can be observed for the benzyl linker series. Compounds **Pro-8** to **Pro-12** show potent degradation of BRD4 with **Pro-11** being the most potent PROTAC with a DC<sub>50</sub> of 1.3 nM and D<sub>max</sub> of 87%. Noteworthy, **Pro-7** is the only PROTAC synthesized with no BRD4 degradation. This is likely again due to the short and very rigid linker used not offering sufficient leeway for ternary complex formation to induce degradation. However, as shown by the CRBN binding data (IC<sub>50</sub>=52.4 nM) and target engagement data (IC<sub>50(live/perme)</sub>=8.4/11.4) **Pro-7** is a PROTAC capable of binding and engaging to CRBN in cells. Interestingly, the observed target engagement for the benzyl linker series **Pro-7** to **Pro-12** does show lower differences in IC<sub>50</sub> between the live and permeabilized cells when compared to the piperidine series. This is likely due to the reduced basicity of the aniline in comparison to the more basic piperidine nitrogen in the piperidine linker series.

Finally, we tested the spirocyclic and heavily rigidified linkers in compounds **Pro-13**, **Pro-14** and **Pro-15**. Although, these PROTACs are fairly similar regarding the degree of rigidification and linker geometry, **Pro-13** turned out to be the most potent degrader from this series with a DC<sub>50</sub> of 0.8 nM

and a  $D_{max}$  of 99%, whereas **Pro-14** and **Pro-15** showed a five-fold difference in potency. While CRBN binding as measured in our TR-FRET assay is again almost identical, a slightly better permeability for **Pro-13** can be observed.

**Table 5:** In-vitro analysis of the synthesized PROTACs. Data for BRD4 degradation, CRBN TR-FRET as well as CRBN target engagement via NanoBRET is shown. Additionally, solubility data at pH 4.5 and 6.8 as well as metabolic stability in mice, rat, and human liver microsomes is given.

Compound	BRD4 Degradation <sup>a</sup> 4 h DC <sub>50</sub> (nM) / D <sub>max</sub> (%)	BRD4 Degradation <sup>a</sup> 18 h DC <sub>50</sub> (nM) / D <sub>max</sub> (%)	CRBN Binding <sup>b</sup> IC <sub>50</sub> (nM)	CRBN Target Engagement <sup>c</sup> IC <sub>50</sub> (nM) live/perm.	Solubility ( $\mu$ g/mL) <sup>d</sup> pH 4.5/6.8	MetStab QH (%) <sup>e</sup> m/r/h
<b>Pro-1</b>	9.1 / 97	3.6 / 98	295.9	301.8 / 215.9	36 / 26	51/34/67
<b>Pro-2</b>	21.1 / 65	11.4 / 80	53.8	388.1 / 17.1	>177 / >162	25/40/68
<b>Pro-3</b>	2.3 / 98	1.1 / 97	41.0	622.1 / 17.8	>185 / >175	27/<23/34
<b>Pro-4</b>	12.8 / 94	2.3 / 96	43.2	291.6 / 14.6	>189 / >175	<24/<23/6 6
<b>Pro-5</b>	1.8 / 97	0.6 / 98	36.6	136.7 / 10.5	>191 / >178	27/<23/54
<b>Pro-6</b>	0.7 / 92	0.3 / 98	36.8	15.3 / 8.9	>197 / >182	<24/<23/5 3
<b>Pro-7</b>	>10000 / -	>10000 / -	52.4	8.4 / 11.7	<1 / <1	25/64/37
<b>Pro-8</b>	>10000 / -	5.7 / 61	57.1	54.6 / 17.7	3 / 1	55/42/86
<b>Pro-9</b>	16.7 / 48	10.6 / 76	72.3	53.6 / 26.0	14 / 4	70/48/>88
<b>Pro-10</b>	>10000 / -	2.8 / 77	59.4	24.9 / 24.9	4 / <1	77/62/>88
<b>Pro-11</b>	2.6 / 62	1.3 / 87	79.2	20.9 / 31.4	6 / <1	76/58/>88
<b>Pro-12</b>	2.0 / 59	1.5 / 82	96.6	18.7 / 31.9	3 / <1	83/66/>88
<b>Pro-13</b>	1.9 / 95	0.8 / 99	55.2	77.0 / 27.5	>190 / 161	44/33/56
<b>Pro-14</b>	11.2 / 99	4.8 / 99	53.8	287.2 / 20.7	>190 / 101	33/<23/60
<b>Pro-15</b>	11.2 / 55	4.6 / 76	37.5	168.7 / 10.1	>188 / >174 <sup>f</sup>	25/<23/41

<sup>a</sup>Degradation of BRD4 measured in HiBiT-BRD4 HEK293 CRISPR cells. <sup>b</sup>TR-FRET CRBN binding assay. <sup>c</sup>NanoBRET target engagement assay. <sup>d</sup>Solubility at pH 4.5 and 6.8. <sup>e</sup>Metabolic stability in mice, rat, human microsomes. <sup>f</sup>Compound not stable under assay conditions.

Next, we turned our attention towards a possible miniaturization of the developed PROTAC synthesis. The aim was to investigate the applicability in high-throughput synthesis settings to allow the generation of PROTAC libraries. We chose to perform the reactions in 1 mL push top glass vials lined with a Teflon septum, as these were compatible with the setup of our photoreactor (see SI for details). The scale of the reaction was reduced from the initially used 0.1 mmol to 25  $\mu$ mol and the conversion to the desired product was determined via LC-MS analysis with an internal standard. For our screening,

we selected five representative linkers from the PROTAC scope in combination with five CRBN aryl bromides. First, we investigated the reproducibility of the setup by comparing the miniaturization results for CRBN aryl bromide **1** with the results obtained in the PROTAC scope (Figure 1, 1<sup>st</sup> column vs. Scheme 3). Gratifyingly, these were in good agreement with the previously isolated yields. We then sought to complete our envisioned PROTAC library by reacting the remaining CRBN aryl bromides **10** - **13** in our miniaturization setup, with the desired products being formed in all cases. Interestingly, piperidinyl based linkers (**L3**, **L5**) resulted in generally higher conversion (26-55%) compared to benzylic ones (**L8**, **L12**; 15-35%), with only slight variations between the different CRBN aryl bromides observed. Spirocyclic linker **L14** showed a higher variability in conversion depending on the CRBN aryl bromide used, with conversions ranging from <15 up to 55%. Overall, these results suggest that the developed one-pot PROTAC synthesis is amenable to a high-throughput synthesis setting, and after further optimization of the operational setup, could be a useful tool in the fast generation of PROTAC libraries.

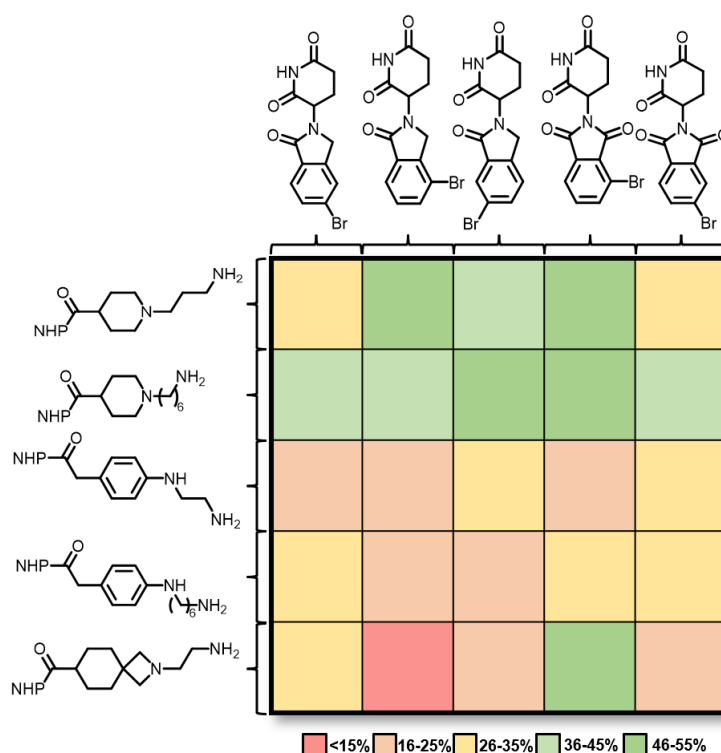


**Figure 1:** Miniaturization and library synthesis of CRBN PROTACs in a one-pot format. Five different CRBN aryl bromides (**1**, **10-13**) were reacted with five different heterobifunctional linkers (**L3**, **L5**, **L8**, **L12**, **L14**). Conversion (%) to the desired product is indicated via a color palette (see supporting information for full details).

## Summary

In summary, we developed a protocol for the one-pot synthesis of PROTACs combining a CRBN E3-ligase binder and (+)-JQ-1 as a POI binder with a library of heterobifunctional linker moieties. The protocol utilizes photoinduced C(sp<sup>2</sup>)-C(sp<sup>3</sup>) cross coupling, followed by amide formation to generate PROTACs in a one-pot fashion with practical yields. The individual transformations of the protocol were optimized in detail and a scope for the C(sp<sup>2</sup>)-C(sp<sup>3</sup>) cross coupling showing 35 examples with yields ranging from 7–93% is given. The one-pot PROTAC synthesis was investigated with various aliphatic, aromatic, and rigidified heterobifunctional linker moieties and 15 PROTACs were successfully synthesized and profiled in cellular degradation assays. 14 out of the 15 generated PROTACs showed pronounced degradation of BRD4, with the most active compound showing activity

in a picomolar range. In addition, a simplistic miniaturization setup was evaluated for the fast generation of a PROTAC library, indicating the compatibility of the developed one-pot transformation in a high-throughput screening process. Overall, the developed method provides rapid access to functional CRBN-PROTACs. We are confident that the reported protocol extends the literature portfolio of PROTAC syntheses via library-based approaches and is of use to current drug discovery programs aiming at the development of CRBN-based protein degraders.

### **Acknowledgements**

The authors would like to thank Christian Salamon, Katharina Mayr, Philipp Toplak, Helmut Berger, Gerhard Gmaschitz, Roland Kousek, Wolfgang Hela, Jessica Linke, Matthias Klemencic, Bernadette Sharps, Romy Schopper, Michael Bieler, Nathalie Harrer and Nina Braun for technical and experimental support, Florian Schiel, Christoph Peinsipp, Stefan Kornigg und Dr. Dietrich Böse for the design and manufacturing of the photoreactor<sup>64</sup>, Tobias Wunberg, Ralph Neumüller, Norbert Kraut, Harald Weinstabl and Darryl McConnell for support of the project and critical feedback.

### **Bibliography**

1. Cromm, P. M. & Crews, C. M. Targeted Protein Degradation: from Chemical Biology to Drug Discovery. *Cell Chem Biol* 24, 1181–1190 (2017).
2. Chamberlain, P. P. & Hamann, L. G. Development of targeted protein degradation therapeutics. *Nat Chem Biol* 15, 937–944 (2019).
3. Hu, Z. & Crews, C. M. Recent Developments in PROTAC-Mediated Protein Degradation: From Bench to Clinic. *Chembiochem* 23, e202100270 (2022).
4. Luh, L. M. *et al.* Prey for the Proteasome: Targeted Protein Degradation—A Medicinal Chemist's Perspective. *Angew. Chem. Int. Ed.* 59, 15448–15466 (2020).
5. Sakamoto, K. M. *et al.* Protacs: Chimeric molecules that target proteins to the Skp1–Cullin–F box complex for ubiquitination and degradation. *Proc National Acad Sci* 98, 8554–8559 (2001).
6. Hughes, S. J., Testa, A., Thompson, N. & Churcher, I. The rise and rise of protein degradation: Opportunities and challenges ahead. *Drug Discov Today* 26, 2889–2897 (2021).
7. Poso, A. The Future of Medicinal Chemistry, PROTAC, and Undruggable Drug Targets. *J Med Chem* 64, 10680–10681 (2021).
8. Troup, R. I., Fallan, C. & Baud, M. G. J. Current strategies for the design of PROTAC linkers: a critical review. *Explor Target Anti-tumor Ther* 1, 273–312 (2020).
9. Hughes, S. J. & Ciulli, A. Molecular recognition of ternary complexes: a new dimension in the structure-guided design of chemical degraders. *Essays Biochem* 61, 505–516 (2017).
10. Kofink, C. *et al.* A selective and orally bioavailable VHL-recruiting PROTAC achieves SMARCA2 degradation in vivo. *Nat Commun* 13, 5969 (2022).

11. Kastl, J. M., Davies, G., Godsman, E. & Holdgate, G. A. Small-Molecule Degraders beyond PROTACs—Challenges and Opportunities. *Slas Discov* 26, 524–533 (2021).
12. Ishida, T. & Ciulli, A. E3 Ligase Ligands for PROTACs: How They Were Found and How to Discover New Ones. *Slas Discov* 26, 484–502 (2020).
13. Wang, C., Zhang, Y., Wu, Y. & Xing, D. Developments of CRBN-based PROTACs as potential therapeutic agents. *Eur J Med Chem* 225, 113749 (2021).
14. Hendrick, C. E. *et al.* Direct-to-Biology Accelerates PROTAC Synthesis and the Evaluation of Linker Effects on Permeability and Degradation. *Acs Med Chem Lett* 13, 1182–1190 (2022).
15. Zheng, S. *et al.* Accelerated rational PROTAC design via deep learning and molecular simulations. *Nat Mach Intell* 4, 739–748 (2022).
16. Li, S., Pissarnitski, D., Nowak, T., Wleklinski, M. & Krska, S. W. Merging Late-Stage Diversification with Solid-Phase Peptide Synthesis Enabled by High-Throughput On-Resin Reaction Screening. *Acs Catal* 12, 3201–3210 (2022).
17. Kammer, L. M. *et al.* Photoredox-Catalyzed Four-Component Reaction for the Synthesis of Complex Secondary Amines. *Org Lett* 22, 3318–3322 (2020).
18. Han, X. *et al.* Strategies toward Discovery of Potent and Orally Bioavailable Proteolysis Targeting Chimera Degraders of Androgen Receptor for the Treatment of Prostate Cancer. *J Med Chem* 64, 12831–12854 (2021).
19. Bhela, I. P. *et al.* A Versatile and Sustainable Multicomponent Platform for the Synthesis of Protein Degraders: Proof-of-Concept Application to BRD4-Degrading PROTACs. *J Med Chem* 65, 15282–15299 (2022).
20. Zhao, W. & Chen, F.-E. One-pot Synthesis and its Practical Application in Pharmaceutical Industry. *Curr Org Synth* 9, 873–897 (2012).
21. Brownsey, D. K., Rowley, B. C., Gorobets, E., Gelfand, B. S. & Derksen, D. J. Rapid synthesis of pomalidomide-conjugates for the development of protein degrader libraries. *Chem Sci* 12, 4519–4525 (2021).
22. Kazantsev, A. & Krasavin, M. Ligands for cereblon: 2017–2021 patent overview. *Expert Opin Ther Pat* 32, 171–190 (2021).
23. Goldberg, F. W., Kettle, J. G., Kogej, T., Perry, M. W. D. & Tomkinson, N. P. Designing novel building blocks is an overlooked strategy to improve compound quality. *Drug Discov Today* 20, 11–17 (2015).
24. Hartung, I. V., Huck, B. R. & Crespo, A. Rules were made to be broken. *Nat Rev Chem* 7, 3–4 (2023).
25. Dunetz, J. R., Magano, J. & Weisenburger, G. A. Large-Scale Applications of Amide Coupling Reagents for the Synthesis of Pharmaceuticals. *Org Process Res Dev* 20, 140–177 (2016).



26. Narayanam, J. M. R. & Stephenson, C. R. J. Visible light photoredox catalysis: applications in organic synthesis. *Chem Soc Rev* 40, 102–113 (2010).
27. Milligan, J. A., Phelan, J. P., Badir, S. O. & Molander, G. A. Alkyl Carbon–Carbon Bond Formation by Nickel/Photoredox Cross-Coupling. *Angew. Chem. Int. Ed.* 58, 6152–6163 (2019).
28. Romero, N. A. & Nicewicz, D. A. Organic Photoredox Catalysis. *Chem Rev* 116, 10075–10166 (2016).
29. Krumb, M. *et al.* Photochemical C–H arylation of heteroarenes for DNA-encoded library synthesis. *Chem Sci* 13, 1023–1029 (2021).
30. Badir, S. O. *et al.* Photoredox-mediated hydroalkylation and hydroarylation of functionalized olefins for DNA-encoded library synthesis. *Chem Sci* 12, 12036–12045 (2021).
31. Lepper, E., Smith, N., Cox, M., Scripture, C. & Figg, W. Thalidomide Metabolism and Hydrolysis: Mechanisms and Implications. *Curr Drug Metab* 7, 677–685 (2006).
32. Reist, M., Carrupt, P.-A., Francotte, E. & Testa, B. Chiral Inversion and Hydrolysis of Thalidomide: Mechanisms and Catalysis by Bases and Serum Albumin, and Chiral Stability of Teratogenic Metabolites. *Chem Res Toxicol* 11, 1521–1528 (1998).
33. Zhou, X.-L. *et al.* A comprehensive review of BET-targeting PROTACs for cancer therapy. *Bioorgan Med Chem* 73, 117033 (2022).
34. Manolikakes, G. Comprehensive Organic Synthesis II (Second Edition). 392–464 (2014) doi:10.1016/b978-0-08-097742-3.00312-8.
35. Dombrowski, A. W. *et al.* Expanding the Medicinal Chemist Toolbox: Comparing Seven C(sp<sup>2</sup>)–C(sp<sup>3</sup>) Cross-Coupling Methods by Library Synthesis. *Acs Med Chem Lett* 11, 597–604 (2020).
36. El-Maiss, J. *et al.* Recent Advances in Metal-Catalyzed Alkyl–Boron (C(sp<sup>3</sup>)–C(sp<sup>2</sup>)) Suzuki–Miyaura Cross-Couplings. *Catalysts* 10, 296 (2020).
37. Xie, J., Jin, H. & Hashmi, A. S. K. The recent achievements of redox-neutral radical C–C cross-coupling enabled by visible-light. *Chem Soc Rev* 46, 5193–5203 (2017).
38. Lopez-Girona, A. *et al.* Cereblon is a direct protein target for immunomodulatory and antiproliferative activities of lenalidomide and pomalidomide. *Leukemia* 26, 2326–2335 (2012).
39. Dreher, S. D., Dormer, P. G., Sandrock, D. L. & Molander, G. A. Efficient Cross-Coupling of Secondary Alkyltrifluoroborates with Aryl Chlorides—Reaction Discovery Using Parallel Microscale Experimentation. *J Am Chem Soc* 130, 9257–9259 (2008).
40. Tellis, J. C., Primer, D. N. & Molander, G. A. Single-electron transmetalation in organoboron cross-coupling by photoredox/nickel dual catalysis. *Science* 345, 433–436 (2014).
41. Zhang, P., Le, C. “Chip” & MacMillan, D. W. C. Silyl Radical Activation of Alkyl Halides in Metallaphotoredox Catalysis: A Unique Pathway for Cross-Electrophile Coupling. *J Am Chem Soc* 138, 8084–8087 (2016).

42. Buzzetti, L., Prieto, A., Roy, S. R. & Melchiorre, P. Radical-Based C–C Bond-Forming Processes Enabled by the Photoexcitation of 4-Alkyl-1,4-dihydropyridines. *Angew Chem-ger Edit* 129, 15235–15239 (2017).
43. Zuo, Z. *et al.* Merging photoredox with nickel catalysis: Coupling of  $\alpha$ -carboxyl  $sp^3$ -carbons with aryl halides. *Science* 345, 437–440 (2014).
44. Kammer, L. M., Badir, S. O., Hu, R.-M. & Molander, G. A. Photoactive electron donor–acceptor complex platform for Ni-mediated C( $sp^3$ )–C( $sp^2$ ) bond formation. *Chem Sci* 12, 5450–5457 (2021).
45. Yang, T., Wei, Y. & Koh, M. J. Photoinduced Nickel-Catalyzed Deaminative Cross-Electrophile Coupling for C( $sp^2$ )–C( $sp^3$ ) and C( $sp^3$ )–C( $sp^3$ ) Bond Formation. *Acs Catal* 11, 6519–6525 (2021).
46. Yi, J., Badir, S. O., Kammer, L. M., Ribagorda, M. & Molander, G. A. Deaminative Reductive Arylation Enabled by Nickel/Photoredox Dual Catalysis. *Org Lett* 21, 3346–3351 (2019).
47. Prier, C. K., Rankic, D. A. & MacMillan, D. W. C. Visible Light Photoredox Catalysis with Transition Metal Complexes: Applications in Organic Synthesis. *Chem Rev* 113, 5322–5363 (2013).
48. Crisenza, G. E. M., Mazzarella, D. & Melchiorre, P. Synthetic Methods Driven by the Photoactivity of Electron Donor–Acceptor Complexes. *J Am Chem Soc* 142, 5461–5476 (2020).
49. Lima, C. G. S., Lima, T. de M., Duarte, M., Jurberg, I. D. & Paixão, M. W. Organic Synthesis Enabled by Light-Irradiation of EDA Complexes: Theoretical Background and Synthetic Applications. *Acs Catal* 6, 1389–1407 (2016).
50. Yuan, M., Song, Z., Badir, S. O., Molander, G. A. & Gutierrez, O. On the Nature of C( $sp^3$ )–C( $sp^2$ ) Bond Formation in Nickel-Catalyzed Tertiary Radical Cross-Couplings: A Case Study of Ni/Photoredox Catalytic Cross-Coupling of Alkyl Radicals and Aryl Halides. *J Am Chem Soc* 142, 7225–7234 (2020).
51. Mann, D. J. & Hase, W. L. Ab Initio Direct Dynamics Study of Cyclopropyl Radical Ring-Opening. *J Am Chem Soc* 124, 3208–3209 (2002).
52. Parsaee, F. *et al.* Radical philicity and its role in selective organic transformations. *Nat Rev Chem* 5, 486–499 (2021).
53. Pryor, W. A. Oxy-Radicals and Related Species: Their Formation, Lifetimes, and Reactions. *Annu Rev Physiol* 48, 657–667 (1986).
54. Galli, C. & Rappoport, Z. Unequivocal SRN1 Route of Vinyl Halides with a Multitude of Competing Pathways: Reactivity and Structure of the Vinyl Radical Intermediate. *Accounts Chem Res* 36, 580–587 (2003).
55. Galli, C., Guarnieri, A., Koch, H., Mencarelli, P. & Rappoport, Z. Effect of Substituents on the Structure of the Vinyl Radical: Calculations and Experiments. *J Org Chem* 62, 4072–4077 (1997).
56. Chan, K.-H., Zengerle, M., Testa, A. & Ciulli, A. Impact of Target Warhead and Linkage Vector on Inducing Protein Degradation: Comparison of Bromodomain and Extra-Terminal (BET) Degraders Derived from Triazolodiazepine (JQ1) and Tetrahydroquinoline (I-BET726) BET Inhibitor Scaffolds. *J Med Chem* 61, 504–513 (2018).

57. Bricelj, A., Steinebach, C., Kuchta, R., Gütschow, M. & Sosič, I. E3 Ligase Ligands in Successful PROTACs: An Overview of Syntheses and Linker Attachment Points. *Front Chem* 9, 707317 (2021).
58. Chan, L. C. & Cox, B. G. Kinetics of Amide Formation through Carbodiimide/N-Hydroxybenzotriazole (HOBt) Couplings. *J Org Chem* 72, 8863–8869 (2007).
59. Mahmoud, K. A., Long, Y., Schatte, G. & Kraatz, H. Rearrangement of the Active Ester Intermediate During HOBt/EDC Amide Coupling. *Eur. J. Inorg. Chem.* 2005, 173–180 (2005).
60. Ghosh, A. K. & Shahabi, D. Synthesis of amide derivatives for electron deficient amines and functionalized carboxylic acids using EDC and DMAP and a catalytic amount of HOBt as the coupling reagents. *Tetrahedron Lett* 63, 152719 (2021).
61. Schwinn, M. K. *et al.* CRISPR-Mediated Tagging of Endogenous Proteins with a Luminescent Peptide. *Acs Chem Biol* 13, 467–474 (2018).
62. Matyskiela, M. E. *et al.* A novel cereblon modulator recruits GSPT1 to the CRL4CRBN ubiquitin ligase. *Nature* 535, 252–257 (2016).
63. Matyskiela, M. E. *et al.* SALL4 mediates teratogenicity as a thalidomide-dependent cereblon substrate. *Nat Chem Biol* 14, 981–987 (2018).
64. Schiel, F., Peinsipp, C., Kornigg, S. & Böse, D. A 3D-Printed Open Access Photoreactor Designed for Versatile Applications in Photoredox- and Photoelectrochemical Synthesis\*\*. *Chemphotochem* 5, 431–437 (2021).